ISSN: 2350-0328

International Journal of Advanced Research in Science, Engineering and Technology

Vol. 4, Issue 2 , February 2017

Resonant Current Control Scheme for the Reduction of Current Harmonics in Grid Connected Photovoltaic Inverters

Gunti Chandu, Sreepriya Vookanti

M.Tech Student, Department of Electrical and Electronics Engineering, SR Engineering College (Autonomous), Warangal, Telangana (India)

Assistant professor, Department of Electrical and Electronics Engineering, SR Engineering College (Autonomous), Warangal, Telangana (India)

ABSTRACT: This paper presents a new control technique used to reduce the harmonic distortion of current, without increasing the computational load of the standard current control abnormal conditions. The proposed control technique overcomes the disadvantages of resonant current control under unbalanced conditions. Simulations results of the proposed control technique are carried out and showed better performance.

KEYWORDS: Distributed generation (DG), photovoltaic (PV), power quality, three-phase inverter.

I. INTRODUCTION

Photovoltaic (PV) power generation is a concept of increasing interest. In recent years, a high number of PV systems with a power capacity up to some megawatts have appeared in the distributed generation (DG) scenario. Usually, these PV systems are connected to the commercial utility grid [1]–[8]. They can also form a microgrid with other DG resources, energy storage systems, and local loads [9]–[10]. Regardless of the output connection, power quality is an essential feature of PV systems. The quality of power is mainly governed by practices and standards on voltage, frequency, and harmonics. In particular, PV systems should have low current harmonic distortion to assure that no adverse effects are caused to other equipment connected to the utility grid or the microgrid.

The resonant current control has been extensively employed to reduce the current harmonic distortion in a wide range of DG applications, including PV systems, wind and water turbines, and fuel-cell inverters. Essentially, this control uses a proportional-resonant (PRES) compensator to track the fundamental component of the current reference signal and a resonant harmonic (RESH) compensator to attenuate the most important current harmonics. Satisfactory results are easily achieved with this control since the resonant compensators are capable of tracking sinusoidal references of arbitrary frequency with zero steady state error. The main problem of the resonant current control is the performance deterioration given by abnormal conditions in the utility grid. In such conditions, grid voltage harmonics and phase imbalances may create current reference signals with non sinusoidal distorted waveforms. Also, grid voltages inter harmonics which often appear in standard variable speed drive applications produce distorted reference signals. As a result, the current harmonic distortion is increased due to precisely the ability of the resonant current control to accurately track the distorted reference waveforms.

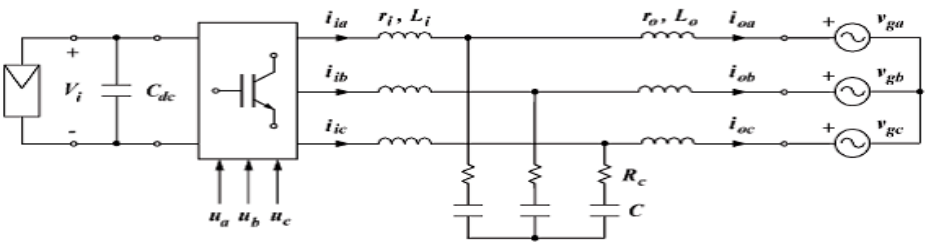

Fig.1. Diagram of the three-phase PV inverter.

ISSN: 2350-0328

International Journal of Advanced Research in Science, Engineering and Technology

Vol. 4, Issue 2 , February 2017

II. THREE-PHASE DG PV INVERTER

Fig. 1 shows the diagram of the three-phase PV inverter. It includes a PV array, a dc-link capacitor, and a three-phase voltage-source inverter. The switches of the inverter are governed by the discrete variables u, which can take the value −1 or 1. Small resistive parasitic elements are considered in this filter. Also, a damping resistor is intentionally introduced in series with the capacitors in order to attenuate the LCL peak magnitude at the resonance frequency. Normally, the losses in this resistor are negligible [1].

A. Open-Loop Model of the Three-Phase PV Inverter

The starting point for the analysis of the resonant current control is an averaged model of the three-phase PV inverter. A circuit representation of this averaged model in the stationary reference frame is shown in Fig.2. The inputs of the model are the dc-link voltage V_i, the grid voltage vg, and the control inputs d, which can take continuous values inside the range

$$-1 \le d_\alpha \le 1 \qquad (1)$$

$$-1 \le d_\beta \le 1. \qquad (2)$$

The outputs of the model are the inverter current i_i and the grid current i_o.

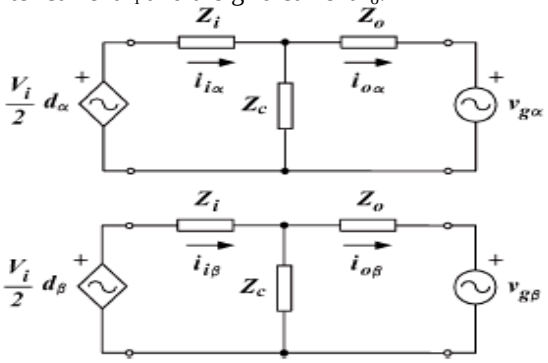

Fig.2. Averaged circuit model of the three-phase PV inverter, where $Z_i(s) = L_i s + r_i$, $Z_o(s) = L_o s + r_o$, $Z_c(s) = 1/(C_s) + R_c$, and s is the Laplace operator.

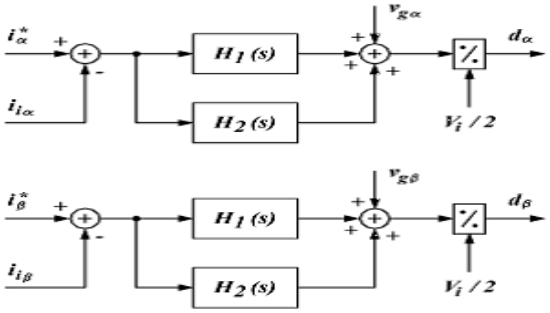

Fig.3. Standard resonant current control in the stationary reference frame.

B. *Resonant Current Control*

Fig. 3 shows the standard configuration of the resonant current control. The error between the inverter current and the reference signal is processed by two compensators connected in parallel: the PRES compensator $H_1(s)$ and the RESH compensator $H_2(s)$. The inverter current is normally employed in the control instead of the grid current. This fact reduces the number of the required current sensors and increases the system robustness [1]. The grid voltage and the dc-link voltage are used as feedforward signals in order to improve the dynamics of the system. The system capability to reject external disturbances is also enhanced with these feedforward signals. From Fig. 3, the control inputs can be written as

$$d_\alpha = \frac{2}{V_i}\left[v_{g\alpha} + (H_1(s) + H_2(s))\,(i_\alpha^* - i_{i\alpha})\right] H_d(s) \qquad (3)$$

$$d_\beta = \frac{2}{V_i}\left[v_{g\beta} + (H_1(s) + H_2(s))\,(i_\beta^* - i_{i\beta})\right] H_d(s). \qquad (4)$$

$H_d(s)$, not shown in Fig. 3, is the transfer function that models the control processing time delay T_d [1]

ISSN: 2350-0328
International Journal of Advanced Research in Science, Engineering and Technology
Vol. 4, Issue 2 , February 2017

$$H_d(s) = e^{-T_d s}. \quad (5)$$

C. *Closed-Loop Model of the Three-Phase PV Inverter*

The analysis of the system can be carried out by means of a closed-loop dynamic model. This model is derived by placing (3) and (4) into the open-loop model shown in Fig. 2, resulting in

$$i_{o\alpha}(s) = G_r(s) i_\alpha^*(s) + G_g(s) v_{g\alpha}(s) \quad (6)$$

$$i_{o\beta}(s) = G_r(s) i_\beta^*(s) + G_g(s) v_{g\beta}(s) \quad (7)$$

where the reference-signal-to-grid-current transfer function and the grid-voltage-to-grid-current transfer function can be expressed, respectively, as

$$G_r(s) = \frac{Z_c(s) G_i(s) \left(H_1(s) + H_2(s)\right) H_d(s)}{1 + T(s)} \quad (8)$$

$$G_g(s) = -\frac{G_i(s) \left(Z_i(s) + \left(H_1(s) + H_2(s)\right) H_d(s)\right)}{1 + T(s)}. \quad (9)$$

Moreover, the loop gain T(s) and the transfer function $G_i(s)$ can be written as

$$T(s) = \left(Z_c(s) + Z_o(s)\right) G_i(s) \times \left(H_1(s) + H_2(s)\right) H_d(s) \quad (10)$$

$$G_i(s) = \frac{1}{Z_i(s) \left(Z_c(s) + Z_o(s)\right) + Z_c(s) Z_o(s)}. \quad (11)$$

It is worth mentioning that the closed-loop dynamics of the grid current does not rely on the dc-link voltage; see (6) and (7). Essentially, this fact can be attributed to the feedforward action introduced in (3) and (4) by the dc-link voltage signal. Note that a feedforward signal of the grid voltage is also included in the control inputs (3) and (4). However, in that case, the closed-loop dynamics of the grid current is directly affected by the grid voltage disturbances through the transfer function $G_g(s)$. As discussed hereinafter, this transfer function presents significant magnitude attenuation in the frequency range of interest. Therefore, the direct influence of the grid voltage disturbances on the grid current is nearly negligible.

III. ANALYSIS AND LIMITATIONS OF THE STANDARD RESONANT CURRENT CONTROL

The standard resonant current control employs two resonant compensators connected in parallel, as shown in Fig. 3 the PRES compensator ensures the correct tracking of the fundamental component of the current reference signal. The RESH compensator attenuates the selected grid current harmonics. Fig. 4 shows the Bode magnitude diagram of the resonant compensators.

$$H_1(s) = k_p + \frac{k_{i1} 2\xi_1 \omega_o s}{s^2 + 2\xi_1 \omega_o s + \omega_o^2} \quad (12)$$

$$H_2(s) = \sum_n \frac{k_{in} 2\xi_n (n\omega_o) s}{s^2 + 2\xi_n (n\omega_o) s + (n\omega_o)^2}. \quad (13)$$

The features of the standard resonant current control emerge from the analysis of the transfer functions (8)–(10). The Bode diagrams of these functions are shown in Fig. 5. Note that the system is stable with a phase margin of 38.4◦ at the crossover frequency of 1.1 kHz; see Fig. 5(a). Moreover, the grid voltage-to-grid-current transfer function $G_g(s)$ has significant magnitude attenuation in the frequency range of interest (i.e., $G_g(s) \rightarrow 0$ in this frequency range); see Fig. 5(b). Thus, from (6), it is easy to observe that the grid voltage disturbances do not directly affect the grid current dynamics. Additionally, the reference-signal-to-grid-current transfer function $G_r(s)$ has a flat 0-dB magnitude within the system bandwidth; see Fig. 5(c). This ensures that the grid current tracks accurately the reference signal, even in the undesired situation in which this signal has significant harmonics. Consequently, from (6), the harmonic distortion present in the reference signal will be transferred to the grid current. The reference signal harmonic distortion may be caused by grid disturbances such as voltage harmonics or imbalances. This is, in fact, an indirect mechanism to increase the output current harmonic distortion through grid voltage disturbances when using the standard resonant current control.

ISSN: 2350-0328

International Journal of Advanced Research in Science, Engineering and Technology

Vol. 4, Issue 2 , February 2017

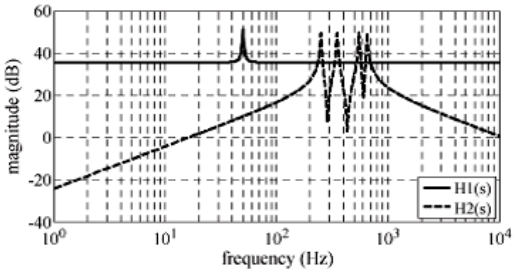

Fig. 4. Bode magnitude diagram of the PRES and RESH compensators employed in the standard resonant current control.

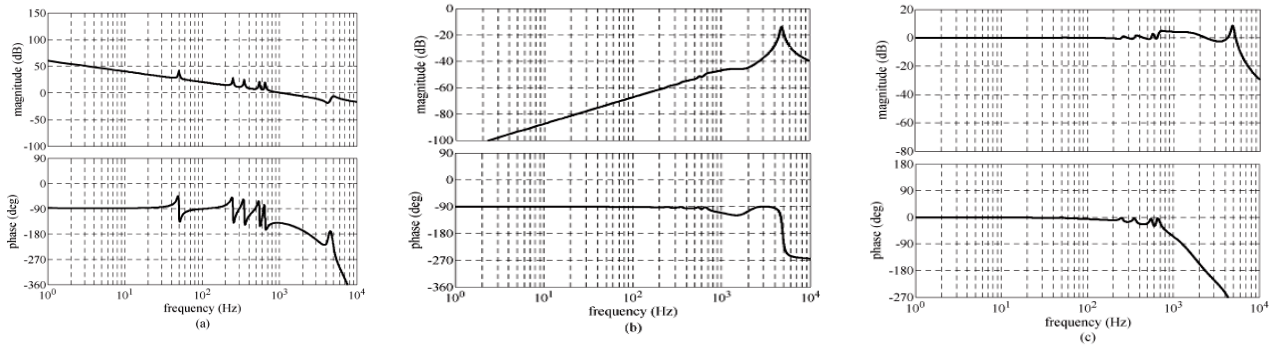

Fig.5. Bode diagrams of the standard resonant current control. (a) Loop gain transfer function T(s), (b) grid-voltage-to-grid-current transfer function $G_g(s)$, and (c) reference-signal-to-grid-current transfer function $G_r(s)$.

IV. PROPOSED RESONANT CURRENT CONTROL

The main objective of the proposed control is to achieve low harmonic distortion in the grid current even during grid abnormal conditions. This feature should be accomplished without increasing the control computational load.

A. *Control Configuration*

Fig. 6 shows the diagram of the proposed control scheme. Note that the configuration is very similar to the standard control shown in Fig. 3. Both the grid voltage and the dc link voltage are included as feedforward signals. The proposed control also has two resonant compensators, but in that case, the input of the compensator located on the bottom is the inverter current instead of the error between this current and the reference signal. This is one of the differences between the standard and the proposed control schemes. The second one is the configuration of the resonant compensators. The control objectives are reached if the resonant compensators are chosen as follows:

$$H_3(s) = \frac{k_{i1} 2\xi_1 \omega_o s}{s^2 + 2\xi_1 \omega_o s + \omega_o^2} \qquad (14)$$

$$H_4(s) = k_p + \sum_n \frac{k_{in} 2\xi_n (n\omega_o) s}{s^2 + 2\xi_n (n\omega_o) s + (n\omega_o)^2}. \qquad (15)$$

Note that the first compensator includes only the fundamental resonant term and the second compensator compresses both the proportional and the harmonic resonant terms. It is worth mentioning that

$$H_1(s) + H_2(s) = H_3(s) + H_4(s) \qquad (16)$$

ISSN: 2350-0328
International Journal of Advanced Research in Science, Engineering and Technology
Vol. 4, Issue 2 , February 2017

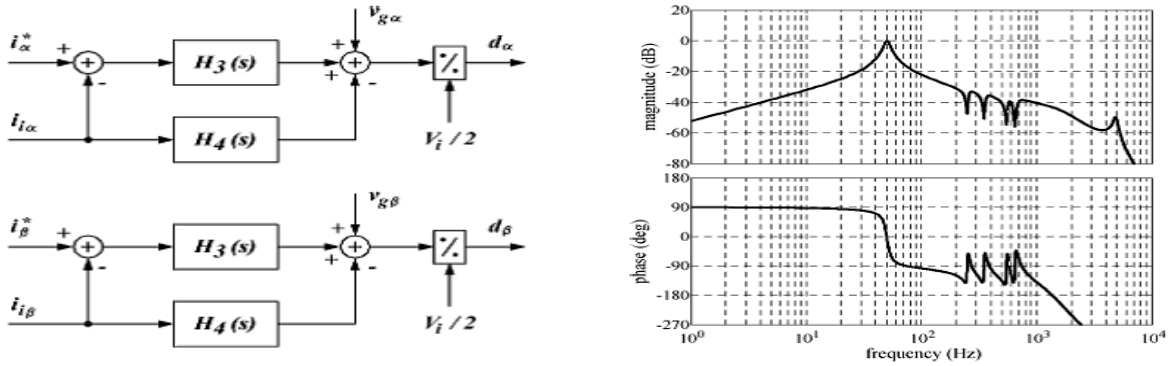

(a) (b)

Fig.6. (a).Proposed resonant current control, (b) Bode diagram of the reference-signal-to-grid-current transfer function for the proposed resonant current control

V. SIMULATION RESULTS

Fig. 7 shows the simulation model of the three-phase grid-connected PV inverter system. This local load is necessary in the setup since the ac source cannot absorb the active power injected by the inverter.

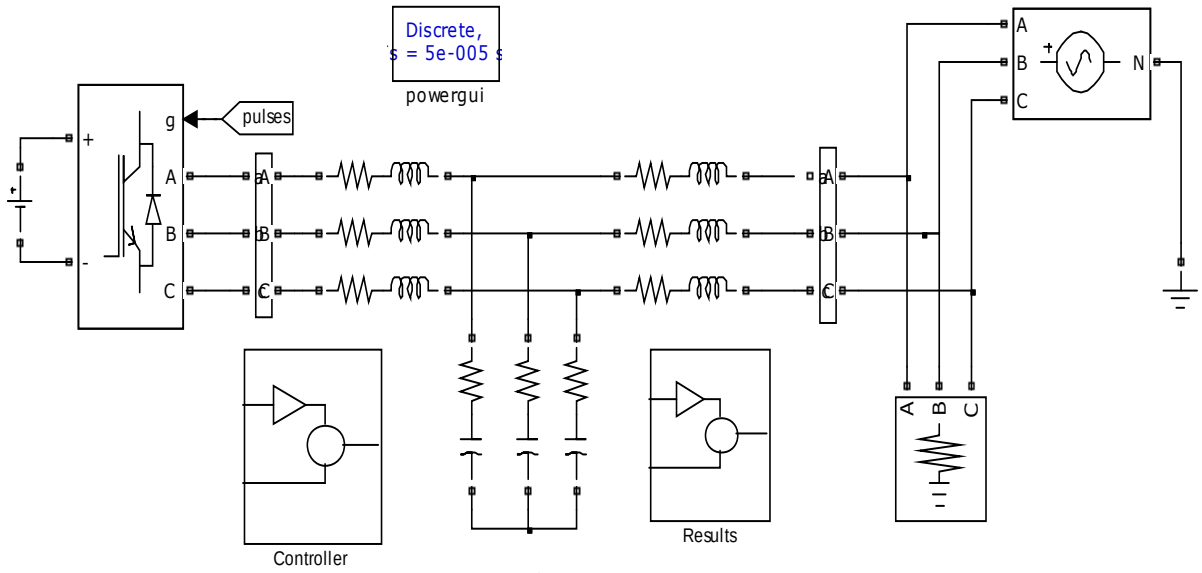

Fig.7 Simulation model of the three-phase grid-connected PV inverter system

A. Current THD Measures

An extensive set of measures has been carried out in order to compare the current harmonic distortion provided by the standard and the proposed control schemes. The Simulation model considers an ideal grid situation, i.e., the voltage supplied by the ac source has both negligible harmonics and no appreciable imbalance. In that situation, the standard and the proposed schemes provide very similar results (not shown here).

ISSN: 2350-0328
International Journal of Advanced Research in Science, Engineering and Technology
Vol. 4, Issue 2 , February 2017

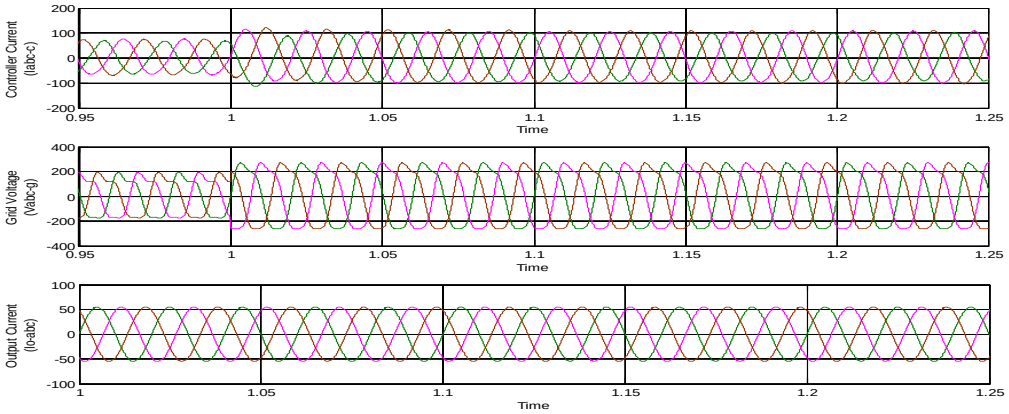

Fig.8. Simulation results of Grid voltage, Inverter current and load current using the standard control without RESH compensator and the standard control with RESH compensator for a grid condition with high voltage THD.

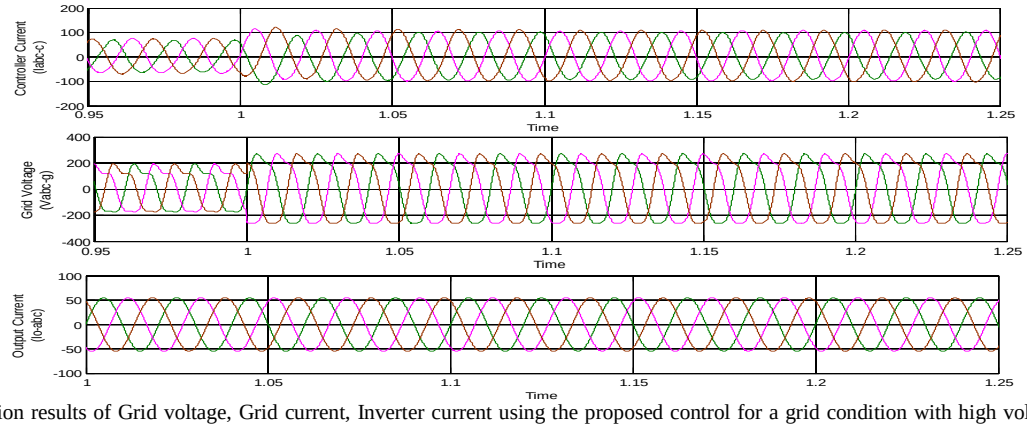

Fig.9. Simulation results of Grid voltage, Grid current, Inverter current using the proposed control for a grid condition with high voltage THD and voltage imbalance.

Fig. 8 and 9 show the Simulation results of Grid voltage, Grid current, Inverter current. Note that the current has experienced an increase due to the reduction of the grid voltage. Basically, the dc-link voltage control loop has enlarged the amplitude of the current reference signals in order to maintain constant the injection of the active power. What is more important is that the standard control produces unsatisfactory results. The current THD of the three phases exceeds the limit even when the RESH compensator is used. On the contrary, the proposed control provides good results. The current THD is low and similar to the value measured when the grid has no voltage imbalance. This feature should be attributed to the ability of the proposed control to eliminate the harmonics present in the current reference signals. It is worth mentioning that the injected currents exhibit a small amplitude mismatch produced by the voltage imbalance. It is expected that this small mismatch has insignificant adverse effects on the power system.

VI. CONCLUSION

The proposed resonant current control of three- phase PV inverters connected to the utility grid in order to attenuate the current harmonics. This controller breaks the disturbance injection mechanism by employing the same compensators that the standard current control uses but inter- connected in a different configuration. The main feature of this controller is to low the current harmonic distortion and low computational load. Simulation of the proposed system is done by using Simulink/Mat-lab. The simulation model is presented in the paper and the results are found to be better.

REFERENCES

[1] E. Figueres, G. Garcerá, J. Sandia, F. González-Espin, and J. C. Rubio, "Sensitivity study of the dynamics of three-phase photovoltaic inverters with an LCL grid filter," IEEE Trans. Ind. Electron., vol. 56, no. 3, pp. 706–717, Mar. 2009.
[2] M. C. Cavalcanti, K. C. de Oliveira, A. M. de Farias, F. A. Neves, G. M. Azevedo, and F. C. Camboim, "Modulation techniques to eliminate

ISSN: 2350-0328

International Journal of Advanced Research in Science, Engineering and Technology

Vol. 4, Issue 2 , February 2017

[3] leakage currents in transformerless three-phase photovoltaic systems," IEEE Trans. Ind. Electron., vol. 57, no. 4, pp. 1360–1368, Apr. 2010.
[4] M. Cacciato, A. Consoli, R. Attanasio, and F. Gennaro, "Soft-switching converter with HF transformer for grid-connected photovoltaic systems,"IEEE Trans. Ind. Electron., vol. 57, no. 5, pp. 1678–1686, May 2010.
[5] S. V. Araujo, P. Zacharias, and R. Mallwitz, "Highly efficient single-phase transformerless inverters for grid-connected photovoltaic systems," IEEE Trans. Ind. Electron., vol. 57, no. 9, pp. 3118–3128, Sep. 2010.
[6] [5] R. Kadri, J. P. Gaubert, and G. Champenois, "An improved maximum power point tracking for photovoltaic grid-connected inverter based-on voltage oriented control," IEEE Trans. Ind. Electron., vol. 58, no. 1, pp. 66–75, Jan. 2011.
[7] A. I. Bratcu, I. Munteanu, S. Bacha, D. Picault, and B. Raison, "Cascaded dc–dc converter photovoltaic systems: Power optimization issues," IEEE Trans. Ind. Electron., vol. 58, no. 2, pp. 403–411, Feb. 2011.
[8] Q. Mai, M. Shan, L. Liu, and J. M. Guerrero, "A novel improved variable step-size incremental-resistance MPPT method for PV systems," IEEE Trans. Ind. Electron., vol. 58, no. 6, pp. 2427–2434, Jun. 2011.
[9] N. A. Rahim, K. Chaniago, and J. Selvaraj, "Single-phase sevenlevel grid-connected inverter for photovoltaic system," IEEE Trans. Ind. Electron., vol. 58, no. 6, pp. 2435–2443, Jun. 2011.
[10] I. J. Balaguer, Q. Lei, S. Yang, U. Supatti, and F. Z. Peng, "Control for grid-connected and intentional islanding operations of distributed power generation," IEEE Trans. Ind. Electron., vol. 58, no. 1, pp. 147–157, Jan. 2011.
[11] J. M. Guerrero, J. C. Vasquez, J. Matas, L. Garcia de Vicuna, and M. Castilla, "Hierarchical control of droop-controlled ac and dc microgrids—A general approach toward standardization," IEEE Trans. Ind. Electron., vol. 58, no. 1, pp. 158–172, Jan. 2011.